



HAL
open science

Gadolinium-based contrast agents: From gadolinium complexes to colloidal systems

Marjorie Yon, Claire Billotey, Jean-Daniel Marty

► **To cite this version:**

Marjorie Yon, Claire Billotey, Jean-Daniel Marty. Gadolinium-based contrast agents: From gadolinium complexes to colloidal systems. *International Journal of Pharmaceutics*, 2019, 569, pp.118577. 10.1016/j.ijpharm.2019.118577 . hal-02318476

HAL Id: hal-02318476

<https://hal.science/hal-02318476>

Submitted on 20 Jul 2022

HAL is a multi-disciplinary open access archive for the deposit and dissemination of scientific research documents, whether they are published or not. The documents may come from teaching and research institutions in France or abroad, or from public or private research centers.

L'archive ouverte pluridisciplinaire **HAL**, est destinée au dépôt et à la diffusion de documents scientifiques de niveau recherche, publiés ou non, émanant des établissements d'enseignement et de recherche français ou étrangers, des laboratoires publics ou privés.



Distributed under a Creative Commons Attribution - NonCommercial 4.0 International License

Gadolinium-based contrast agents: from gadolinium complexes to colloidal systems.

Marjorie Yon^a, Claire Billotey^b, Jean-Daniel Marty^{a,*}

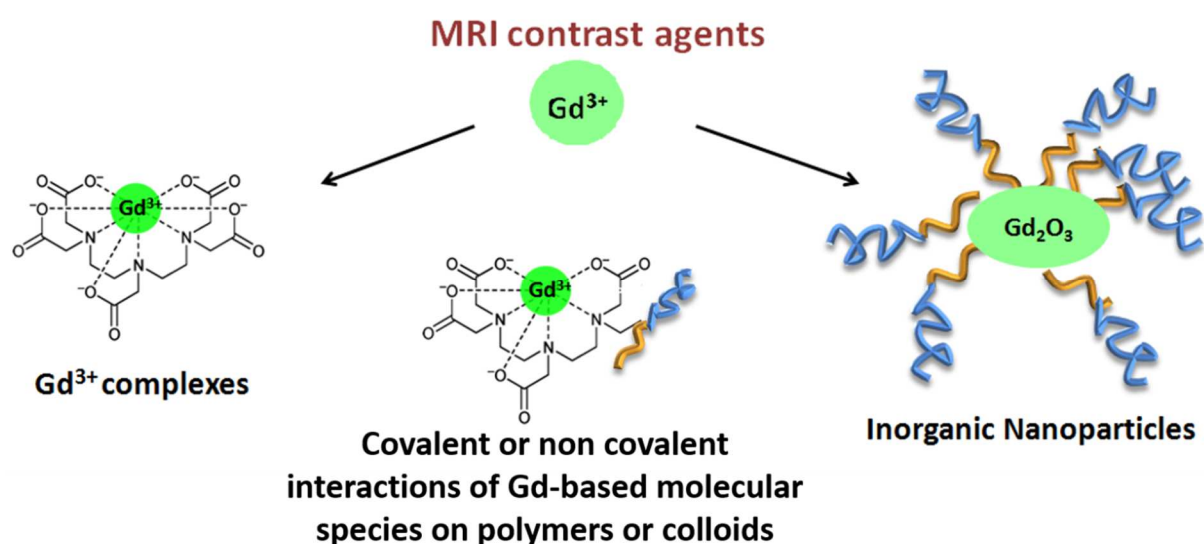
^a Laboratoire des IMRCP, Université de Toulouse, CNRS UMR 5623, Université Paul Sabatier, 118, route de Narbonne 31062 Toulouse Cedex 9, France

^b EMR 3738 Ciblage Thérapeutique en Oncologie, Université de Lyon, Université Jean Monnet, Hospices Civils de Lyon, 42023 Saint-Etienne Cedex 2, France

* corresponding author : E-mail: marty@chimie.ups-tlse.fr

Abstract: Nowadays, most of the clinically used contrast agents are based on the use of gadolinium molecular complexes like Dotarem®, Magnevist®.... Nevertheless, developing new gadolinium based contrast agents with enhanced relaxivity properties while avoiding gadolinium release in human tissue is still of paramount importance. We describe here two promising families of contrast agents which meets these criteria and compared their properties to the ones of clinically used Gd complexes. The first one is based on contrast agents obtained by covalent or non-covalent interactions of gadolinium molecular complexes with polymers, nanoparticles or liposomes. The second family is based on the formation of gadolinium particles (Gd_2O_3 , $GdPO_4$, $NaGdF_4$, $GdF_3...$) of controlled morphology and composition. The performance of these two families is described as well as their development perspective.

Graphical abstract:



Keywords: Magnetic resonance imaging, MRI, gadolinium, relaxivity, hybrid polyion complexes, gadolinium nanoparticles

Introduction

Magnetic resonance imaging (MRI) is a powerful medical diagnostic tool (Mansfield and Maudsley, 1976) whose efficiency is greatly improved by the use of exogenous contrast agents (CAs) (Patten et al. 1993, Caravan, 2006). The two most common classes of contrast agents are: (a) T1 or positive contrast agents that shorten proton longitudinal or spin lattice relaxation time and (b) T2 or negative contrast agents that shorten proton transversal or spin-spin relaxation time (Young et al., 1981). Whereas superparamagnetic iron oxide nanoparticles are most widely studied as T2 agents, CAs based on the lanthanide ions Gd^{3+} are most often employed as T1 agents. Indeed, gadolinium, a lanthanide metal ion with seven unpaired electrons, has demonstrated its efficiency in enhancing proton relaxation because of its high magnetic moment and paramagnetic properties and its ability to coordinate water efficiently. However, the toxicity of Gd ions related to their substitution or antagonist activity of calcium in a variety of cellular reactions (Das et al., 1988) or in the occurrence of nephrogenic systemic fibrosis (Sieber et al., 2008) prevents its direct administration. Therefore to limit the cytotoxicity of Gd ions in commercially available CAs, Gd ions are chelated by specific interacting structures like linear multifunctional or macrocycles structure (Figure 1).

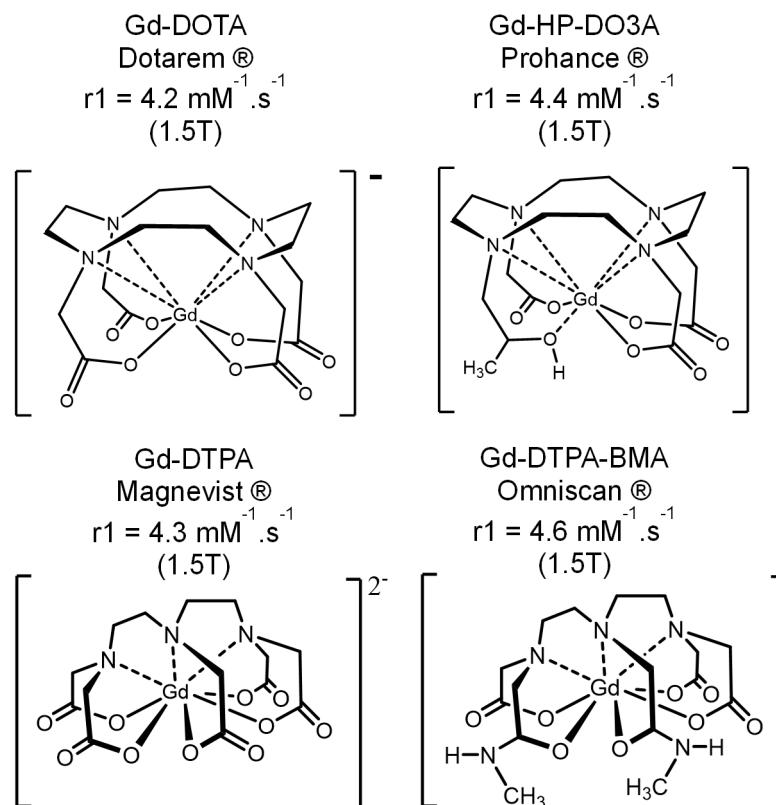


Figure 1. Gd-DOTA, Gd-DTPA, Gd-HP-DO3A and Gd-DTPA-BMA chemical structures. Adapted from (Hermann et al., 2008).

The first families of Gd-based CAs were using linear complexing molecules. In 1987, Gd-diethylenetriamine pentaacetic acid (Gd-DTPA, MAGNEVIST®) (Harpur et al., 1993; Weinmann et al., 1984) was proposed for clinical uses. Then three other linear Gd-based CAs were further approved until 2004: Gd-DTPA, gadodiamide - OMNISCAN® (Radbruch, A. et al., 1987, Schmiedl, U., 1987), gadopentetate dimeglumine (OPTIMARK®) and gadobenate dimeglumine (MultiHance®),(Johansson et al., 2012). In addition, macrocyclic Gd-based CAs (gadoteridol, Gd-tetraazacyclododecanetetraacetic acid and gadobutrol) were also developed to limit the release of free Gd ions and were authorized by several regulatory health agencies since 1994 as commercial products (PROHANCE®, DOTAREM®, GADAVIST®). Interestingly, these macrocyclic Gd-based CA enables to observe a lower level of remaining Gd in vivo in comparison to their linear counterpart (Gibby W.A. et al., 2004). Nevertheless, molecular complexes possess limitations, such as residual toxicity (Kanda et al., 2014, Kanda et al., 2015, Radbruch et al., 2015) and reduced efficiency at the higher magnetic fields of modern MRI instruments. This compels the main regulatory health agency in 2017 to control more carefully the use of this kind of contrast agents and European medicine agency suspended the authorization of the intravenous linear Gd-based CAs.

Current challenge is to develop new Gd-based CAs that avoid the release of the free Gd ions to prevent further complications. At the same time there is still a need of Gd-based CAs with enhanced relaxation properties to decrease the amount of injected compound. To reach such a goal colloidal CAs are of special interest. Indeed the use of Gd-based colloidal structures in the 10 to 100 nm size range enable first to increase the relaxivity of obtained CAs. This effect is related to a much slower tumbling effect compared to molecular gadolinium complexes induced by a huge increase in the molecular weight of the gadolinium species (and of hydrodynamic radius). Slowing tumbling induces higher relaxivity. Gd ions located within the colloidal species will rotate at the same (and very low) rate than the whole NPs, increasing the observed relaxivity. Therefore lower injected levels are permitted. Moreover, colloidal structures present some additional features concerning their stability that make them candidate of choice for new families of CAs. In this review, we will present two different families of enhanced colloidal Gd-based CAs (Figure 2): 1) gadolinium complexes grafted or in interaction onto colloidal structures, 2) inorganic nanoparticles of controlled shape and properly functionalized.

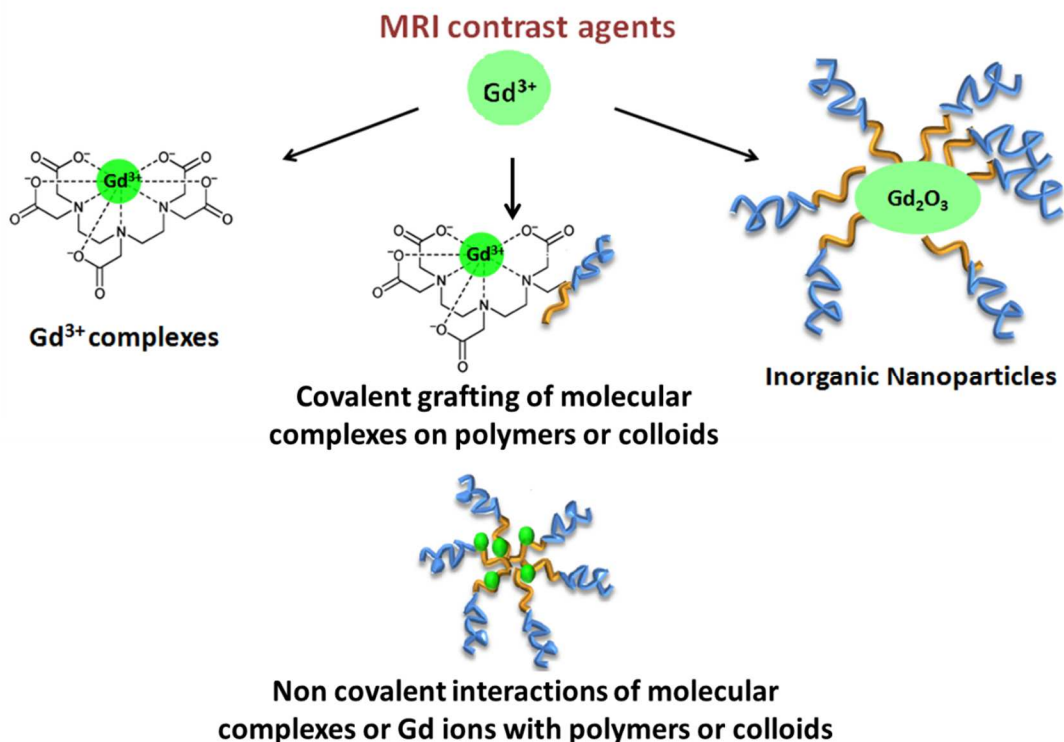
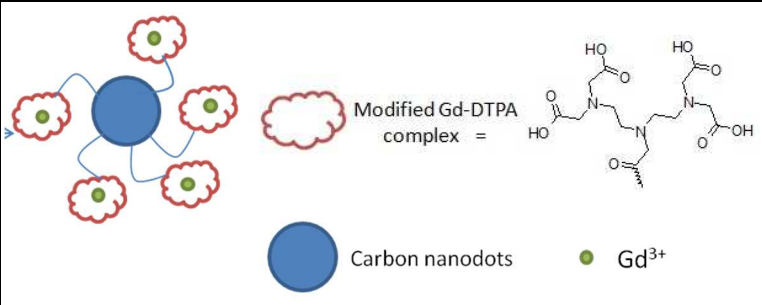
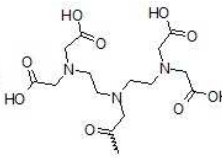


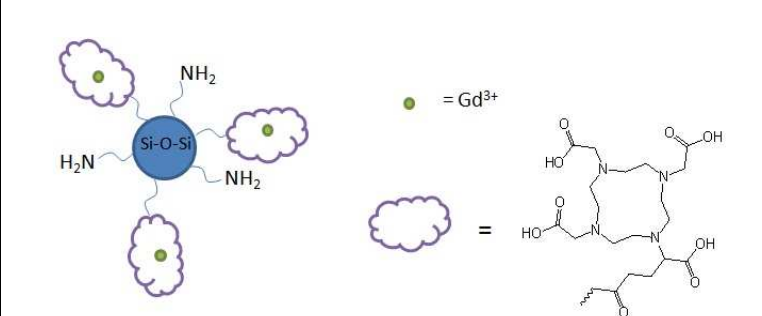


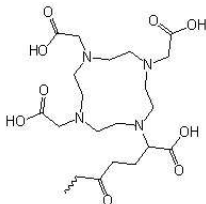
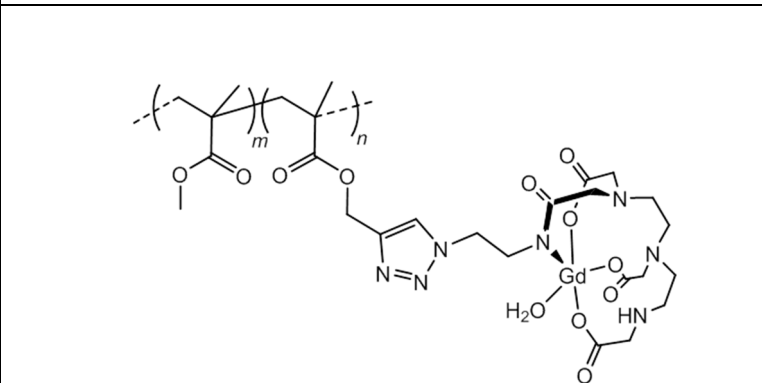
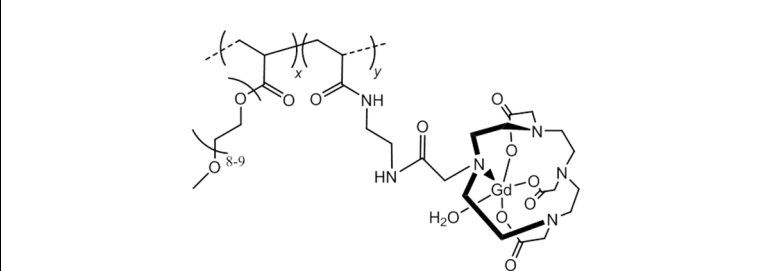


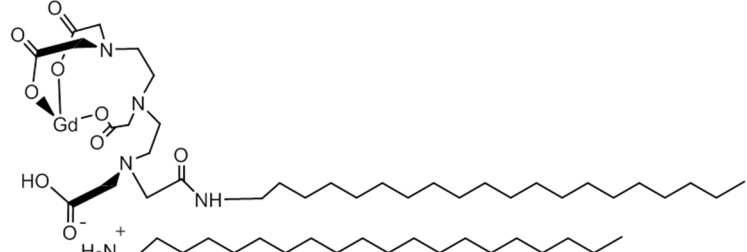
Figure 2. Main families of Gd-based contrast agent.

1. Contrast agents based on covalent or non-covalent grafting of gadolinium complexes on polymer or colloidal structures.

1.1. Grafting of gadolinium complexes. The structure of clinically used low molecular weight Gd-based CAs is presented in Figure 1. As can be seen Gd ions are interacting specifically with chelating agents in the form of macrocycles or linear ligands. Whereas those chelating agents enable to minimize ion exchange with competing ions, they also tend to decrease the amount of water molecules in direct interaction with Gd. Hence, at a same magnetic field value of 0.5T, relaxivity of free gadolinium is about $7 \text{ mM}^{-1} \cdot \text{s}^{-1}$ against $3.8 \text{ mM}^{-1} \cdot \text{s}^{-1}$ when the ion is chelated by DTPA through specific interaction, at 37°C (Villaraza et al., 2010). This results in a relative poor efficiency of this CAs. Moreover, 90% of the product is out of the body in less than an hour through renal filtration and vessel leakage, which let short time to these species to act as CAs and necessitate the injection of high amount of CAs. The aim thus is to optimize the pharmacokinetic of Gd-based CA and to increase the relaxivity value of these CAs. To this purpose, chelating agents are grafted to polymer chains, colloids or lipids. Immobilization of Gd-complexes enable to reduce the tumbling rate by slowing down rotational motions and thus provides higher relaxation times. (Du et al., 2018). The attachment of several complexes on macromolecules, colloids or lipids thereby increases relaxivity value and thus permits to decrease the administration dose. Table 1 presents some typical examples of CAs developed by using such a strategy.

Table 1. Typical examples of gadolinium complexes grafted on colloidal structures.

Structure	r_1 relaxivity in $\text{mM}^{-1}\cdot\text{s}^{-1}$ (magnetic field)	Size (nm)	Reference
 <p>Modified Gd-DTPA complex = </p> <p>Carbon nanodots  Gd^{3+} </p>	8.05 (3T)	100	Ding et al., 2014
 <p>Si-O-Si NH_2 H_2N NH_2</p> <p> = Gd^{3+}</p> <p> = </p>	17.97 (1.5T)	4,5	Tran et al., 2018
	NG	NG	Younis et al., 2016
	Linear 15.6 (0,5T)	NG	Li et al., 2012
	Hyperbranched 15,4 (0,5T)	8-9	
	Star 13,5 (0,5T)	16	

	NG	440	Kabalka et al., 1987
---	----	-----	----------------------

*N.G : Not given

We will describe here some typical examples of the main families of colloidal systems. For a more complete description, Villaraza et al. (2010) reviewed the manifold types of colloidal systems (e.g. dendrimers, micelles, proteins, liposomes) tailored with Gd complexes.

Du et al. described the grafting of DTPA complexes onto carbon nanodots (Ding et al., 2014; Du et al., 2018). For this, after the protection of 4 of its 5 carboxylic acid functions, protected DTPA was reacted with the amine functions located on the surface of carbon nanodots (Figure 3). After a deprotection step, the modified particles complexed gadolinium ions to form a colloidal contrast agent. These supported CAs had several advantages compared to Gd-DTPA complexes: increased relaxivities (r_1 value of $8 \text{ mM}^{-1}\cdot\text{s}^{-1}$ compared to $4 \text{ mM}^{-1}\cdot\text{s}^{-1}$ for the Gd-DTPA at a 3T magnetic field) and an ability to interact more easily with cancer cells thanks to enhanced permeability and retention effect. In addition the fluorescence of the carbon nanodots provided another way to image the glioma, making the CAs dual-imaging species.

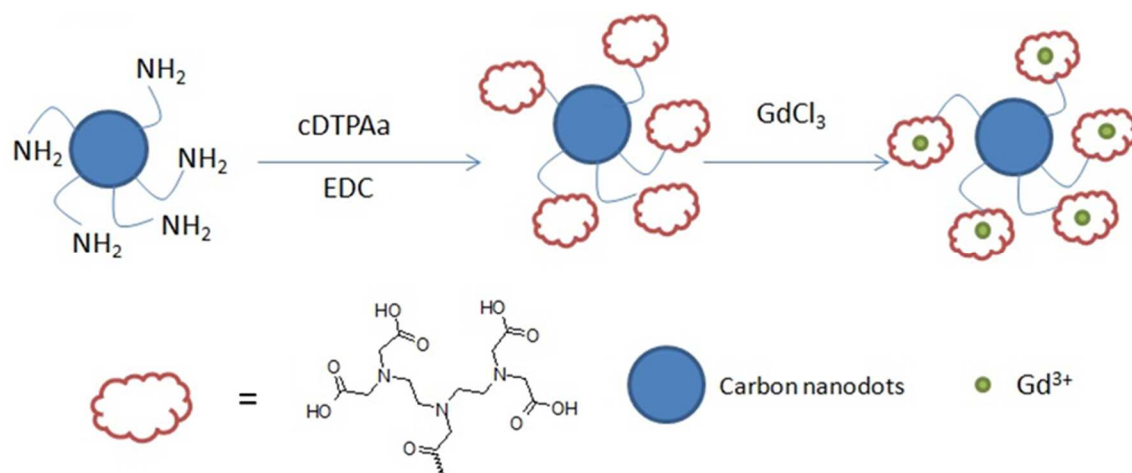


Figure 3. Preparation of modified carbon nanodots with clinical Gd-DTPA in a two-step process: 1) coupling of amino group on the surface of carbon nanodots with protected DTPA (cDTPAa) thanks to 1-ethyl-3-(3-dimethylaminopropyl)carbodiimide (EDC) coupling agent and deprotection 2) complexation with gadolinium ions. Adapted from references (Du et al., 2018).

Another strategy to obtain Gd complexes grafted onto colloidal structures was described by Tran et al. (2018) by using a DOTA properly modified with a terminal triethoxy group as illustrated in Table 1. Siloxane nanoparticles covered by DOTA were then obtained by using sol gel chemistry. At a 1.5 T magnetic field, these particles had higher longitudinal relaxivity value than for free Gd-DOTA complexes, i.e $r_1=18 \text{ mM}^{-1}.\text{s}^{-1}$ and $4.2 \text{ mM}^{-1}.\text{s}^{-1}$ respectively. Further association with ^{64}Cu enabled to use these particles as multimodal agents for MRI and PET imaging techniques. The biodistribution revealed that they were rapidly eliminated in the kidney.

Relaxation properties of gadolinium complexes can also be improved by grafting them onto macromolecules. Hence, Younis et al. (2016) grafted Gd-DTPA complex on poly(methyl)methacrylate-co-propargylmethacrylate to obtain Gd-DTPA-PMMA nanoparticles (see structure in Table 1). Different amounts of Gd-DTPA were incorporated with the PMMA polymer chains. This enable to test the influence of the Gd concentration on the contrast obtained at a 7T magnetic field. Interestingly, magnetic resonance images showed that the contrast was not significantly improved by increasing the amount of gadolinium and that low amount of gadolinium ions were sufficient to obtain good contrast properties. In addition these modified polymers showed a good stability through low gadolinium leakage in PBS buffer at 37°C during 90 days. Li et al. (2012) studied the influence of macromolecular architecture on relaxivity with linear, hyperbranched and star copolymer grafted with DO3A contrast agent (See Figure 4A).

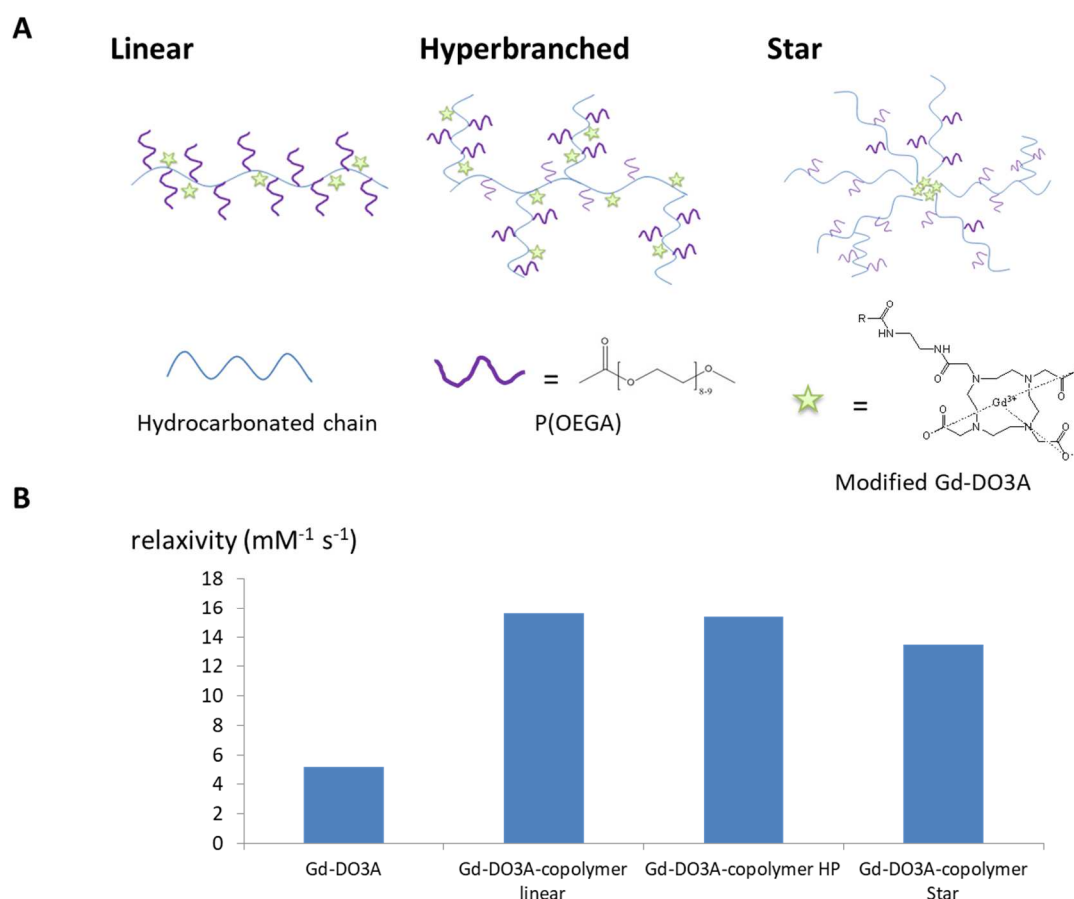


Figure 4. A. Chemical structure of linear, hyperbranched and star polymers P(OEGA-co-PFPA) with grafted DO3A contrast agents. B. Longitudinal relaxivity value for the single chelating agent and for the three architectures of the dendrimer. Adapted from reference (Li et al., 2012).

As shown in Figure 4B, a significant increase of relaxivity was measured for grafted Gd-DO3A complex compared to the relaxivity of free complex whatever the architecture of polymer is. Moreover the authors evidenced the role of each architecture on molecular tumbling and water exchange rate. They highlighted that, in the case of the star shape copolymer, the polymer shell reduced the diffusion of water molecules near the core-located Gd complexes which induced a decrease of relaxation rate compared to linear or hyperbranched architectures. Hence, despite the globular aspect of the hyperbranched structure, the mobility of gadolinium ion inside the macromolecular architecture was the same than for the linear one, proving the very low influence of the hydrodynamic radii of the molecule. In addition to the architecture, average molecular weight of the chosen polymer can also play a role on relaxation properties. To study this, Margeruma et al. (1997) studied polyamido(amine) (PAMAM) dendrimers of different generation of a structure comprising Gd-DO3A CAs. An increase of relaxivity was observed when the molecular weight of the polymer increased due to slower molecular tumbling: from 14.8, to 16.9 and 18.8 $\text{mM}^{-1}\cdot\text{s}^{-1}$ for PAMAM polymer of 3rd; 4th and 5th generation respectively. However Bryant et al. (1999)

evidenced a saturation limit for PAMAM of 7th generation and explained this phenomenon with the stagnation of the water exchange rate.

In order to enhance relaxivity properties, apart from nanoparticles and polymer structures, Gd-complexes can also be covalently linked to lipid. These modified lipids can be inserted in liposome structures made of phospholipids that presents low toxicity. Kabalka et al. (1987) have introduced modified Gd-DTPA (see structure in Table 1) in liposome structures with an overall size of 440 nm. As expected, a higher relaxivity is observed for liposomic structures compared to GD-DTPA. Interestingly, the ability to insert increasing amount of Gd complex in the liposome structure enabled to measure an increase of relaxivity of the vesicular specie up to a content of 33,3%. The biodistribution of these contrast agents indicated that the liposomes are rapidly removed from blood and degraded in the liver by Kupffer cells. Another interesting application of those structures is to combine different functionalities like luminescence, magnetic or targeting in one particle. Skupin-Mrugalska et al. (2018) combined a model photosensitizer for photodynamic therapy, zinc phtalocyanine, and a MRI Gd-based contrast agent based on Gd-DTPA modified with a lipophilic chain. Studies proved that Gd did not hamper the photosensitizing ability of the zinc specie. Moreover, comparisons between liposomes comprising or not zinc phtalocyanine showed that the presence of the photosensitizer enhance relaxivity properties of these Gd-based CAs. At low magnetic field (16,5 MHz) high r_1 values up to $50 \text{ mM}^{-1}\cdot\text{s}^{-1}$ were found, whereas at high magnetic field (400 MHz), r_2 values up to $90 \text{ mM}^{-1}\cdot\text{s}^{-1}$ were measured. Lastly, liposomes can be considered as nanocarriers, which can participate to active targeting strategies by a lipophilic chain bearing a specific probe. Furthermore, the following of this targeting with MRI device would inform on the pathway of the agent towards the target. To this end, Yoo et al. (2016) designed fibrin-binding, peptide amphiphile micelles by incorporating at different concentration a targeting peptide cysteine-arginine-glutamic acid-lysine-alanine (CREKA) with amphiphilic molecules containing Gd-DTPA complex. Besides, the targeting particles were compared to non targeting ones. Whereas in vitro studies confirmed that a uniform amphiphile backbone and micelle shape homogeneity had a large contribution to the clot-targeting capability, in vivo studies showed fibrin specificity was conferred by the peptide ligand without much difference between the nanoparticle formulations.

1.2. From gadolinium specific complexes to hybrid polyion complexes

Hence, immobilization of Gd-chelates onto macromolecules or nano-objects is one efficient way to provide more efficient relaxation by slowing down rotational motion, although the synthetic pathways to such modified polymers can be complicated. An alternative to these strategies is to induce the formation of aggregates (also called coacervates or hybrid polyion complexes, HPICs) between metal ions and block copolymers bearing more simple but non-specific functional groups (Figure 5). This was done for example by Wang et al. (2013) where a negatively charged Gd complex interacted with a diblock cationic copolymer. Another alternative is the use of uncomplexed gadolinium ions which will interact with polymers

functionalized by multidentate groups (Figure 5). (Wang et al., 2012; Wang et al., 2015; Cao et al., 2015)

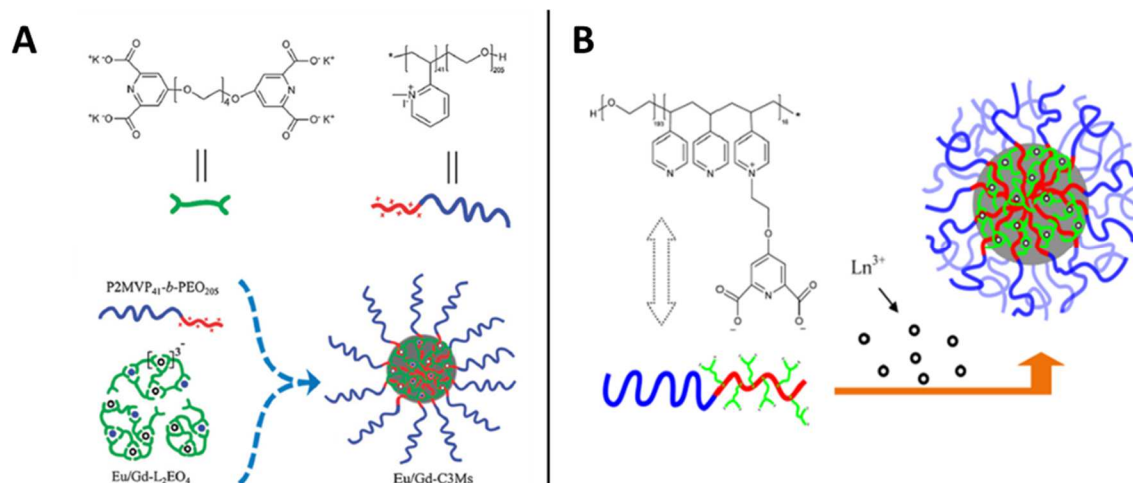


Figure 5. Related strategies leading to the formation of CAs from the interaction of A) charged block copolymers with lanthanides complexes (Wang et al., 2013) or B) block copolymers comprising multidentate complexing groups with lanthanide ions.(Wang et al., 2012). Adapted from references (Wang et al., 2013) and (Wang et al., 2012).

Nevertheless, both examples involve gadolinium-chelating groups with complex structures. New, less complex strategies could allow the easy development of a new generation of CAs. Thus, HPICs obtained from the addition of simple charged polyvalent metal ions (e.g. Cu²⁺, Zn²⁺) to a solution of double hydrophilic block copolymers with generic functions that are not specifically designed for metal ions could be of great interest. Recently it was demonstrated that gadolinium-containing HPICs prepared (see Figure 6) from a commercially available diblock copolymer made of poly(acrylic acid), PAA, and poly(ethylene oxide), PEO, blocks exhibited exceptionally high stability upon dilution.

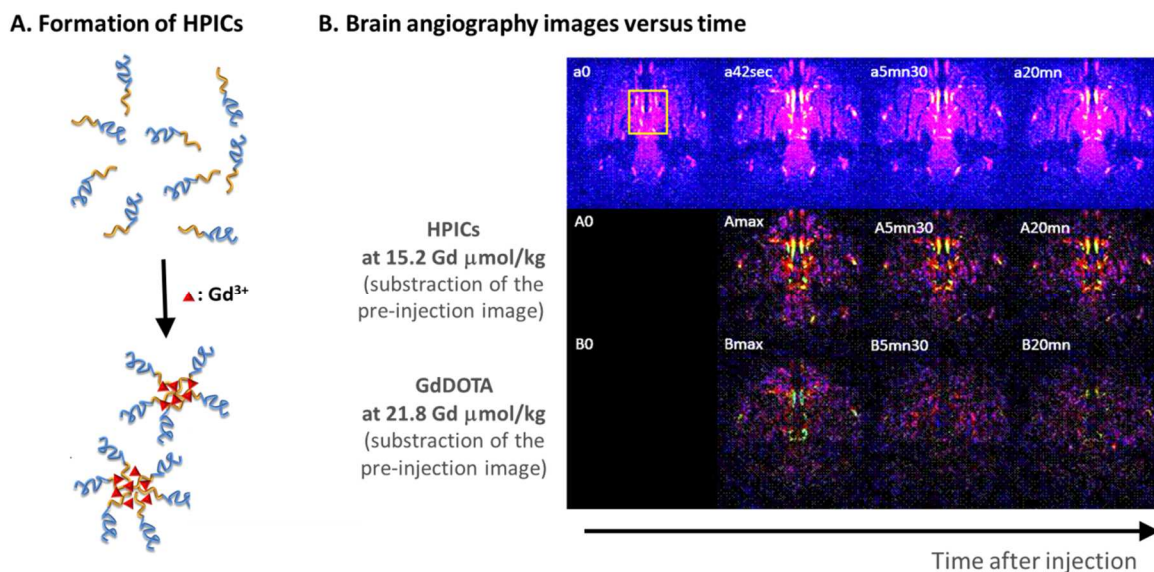


Figure 6. A. The addition of gadolinium ions to a double hydrophilic block copolymer forms polymeric nanoparticles called hybrid polyion complexes HPICs (in yellow-orange: ionizable block; in dark blue: neutral block). B. Brain angiography images versus time obtained with contrast agent based on HPICs compared to Gd-DOTA clinically available contrast agent. Adapted from reference (Frangville et al., 2016).

Indeed, at a magnetic field of 7T, the hybrid polyion complex, with a mean diameter ca 20 nm, exhibited a longitudinal relaxivity of $15.4 \text{ mM}^{-1}\cdot\text{s}^{-1}$, against $4.1 \text{ mM}^{-1}\cdot\text{s}^{-1}$ in the same conditions for Gd-DOTA and $8.8 \text{ mM}^{-1}\cdot\text{s}^{-1}$ for hybrid gadolinium oxide nanoparticles. Moreover, the *in vivo* study showed a pretty long blood remanence, followed by a fast urinary elimination. These systems were combining a low gadolinium quantity with a high relaxation signal, meeting with the initial requirements based on a limited release of free gadolinium within the tissues and enhanced relaxation properties (Frangville et al., 2016; Mingotaud et al., 2017).

2. Inorganic Nanoparticles.

In order to minimize the *in vivo* release of gadolinium ion, many studies have proposed the use of gadolinium-based nanoparticles. In addition there are numerous advantages to nanoparticle-based agents including easy surface modification for incorporating specific vectors and the opportunity to combine properties to give multimodal agents. (Cheng Y. et al., 2014; Cheng Z. et al., 2014). Hence, recent reports have described NPs of gadolinium oxides (Bridot et al., 2007 ; Park et al., 2009 ; Das et al., 2010 ; Faucher et al., 2012), fluorides (Evanics et al., 2006 ; Xu et al., 2014) or phosphates (Lessing and Erickson, 2003; Fang et al., 2003; Hifumi et al., 2006; Hifumi et al., 2009; Ren et al., 2012; Dumont et al., 2012; Rodriguez-Liviano et al., 2013). However, the use of these nanoparticles as contrast agents is still dependent on the production of nanoparticles of well controlled size and morphology,

the relaxation properties being highly dependent on these parameters as has been suggested for Gd₂O₃ NPs although with different surface coatings (Park et al., 2009). Moreover, the particles require suitable coatings, such as organic ligands or polymers to improve their biocompatibility, reduce their toxicity and raise the interaction with water molecules. .

2.1. Control of nanoparticle size and effect on relaxivity properties.

As just mentioned, the control of NPs size is required to have access to NPs with reproducible relaxivity property. Therefore a tremendous amount of work was dedicated to the development of synthetic method to get access to stable nanoparticle with controlled size and morphology. Gadolinium oxides (Gd₂O₃), fluorides (GdF₃, NaGdF₄) or phosphates (GdPO₄) have been described in literature, are obtained by precipitation reaction in presence of well-chosen stabilizing/agent. These hybrid materials offer relaxivities per mole of Gd comparable or superior to the common molecular agents. Among them, gadolinium phosphate nanoparticles (GdPO₄ NPs) are of special interest because of the combination of low solubility, ease of surface modification, and the variety of synthetic routes available to form particles. (Liu and Byrne, 1997) Hydrothermal synthesis (Hifumi et al., 2006; Hifumi et al., 2009; Ren et al., 2012; Laudise and Ballman, 1958; Hikichi et al., 1978) and more recently microemulsion synthesis (Dumont et al., 2012) or a templated mineralization process (Du et al., 2015) were used to form well-defined GdPO₄ NPs as nanorods or nanowires of tens to hundreds nanometers length. Interestingly, nanoparticles of GdPO₄, or even particles with GdPO₄ modified-surfaces, have been shown to be compatible with biological media. For example, Li et al. (2014) demonstrated that pretreatment of rare earth oxide nanoparticles with phosphate, protects against *in vivo* biological interference of gadolinium ions with Ca²⁺ involved in cell metabolism as well as pro-fibrogenic effects favored by the presence of Gd³⁺ ions. This result was further supported by cell toxicity and *in vivo* experimental assays performed with dextran-coated GdPO₄ NPs that showed no impact on cell viability, observed over long residence times in plasma. (Hifumi et al., 2006; Hifumi et al., 2009) Synthesis pathways to obtain nanometrically controlled particle sizes have thus been developed through the use of different polymer families of different architectures: block polymers, branched polymers. These polymers act as both a growth limiter during the growth process of nanoparticle and a stabilizer to provide increased colloidal stability in biological environments: As a first step, Gd³⁺ was sequestered within the polymer and then GdPO₄ NPs were obtained after a precipitation step induced by the addition of phosphate ions. In these conditions final NPs structure will depend strongly on the polymer architecture and on the concentration of reactant in solution. Playing with the mixing speed also allows to obtain particles of a better controlled size. In that context ionic nanoprecipitation is of special interest (Figure 7): it involves the rapid mixing of a water stream containing Gd³⁺ ions with one containing stabilizing agent and phosphonate ions in a confined impinging jet mixer or multi-inlet vortex mixer. Rapid mixing assures homogeneous supersaturation prior to

nucleation, growth and aggregation events, and the diffusion-limited assembly driven by ionic interactions results in particles with narrow size distributions. The particle growth is arrested by the adsorption of the polymer onto the NP surface resulting in the formation of a dense, stabilizing corona. (Pinkerton et al., 2017) GdPO_4 and $\text{Gd}_x\text{Eu}_{1-x}\text{PO}_4$ NPs in the 20 to 100 nm range were thus obtained with relaxivity values r_1 and r_2 in the $15\text{--}40\text{ mM}^{-1}\cdot\text{s}^{-1}$ range at 1.4 T.

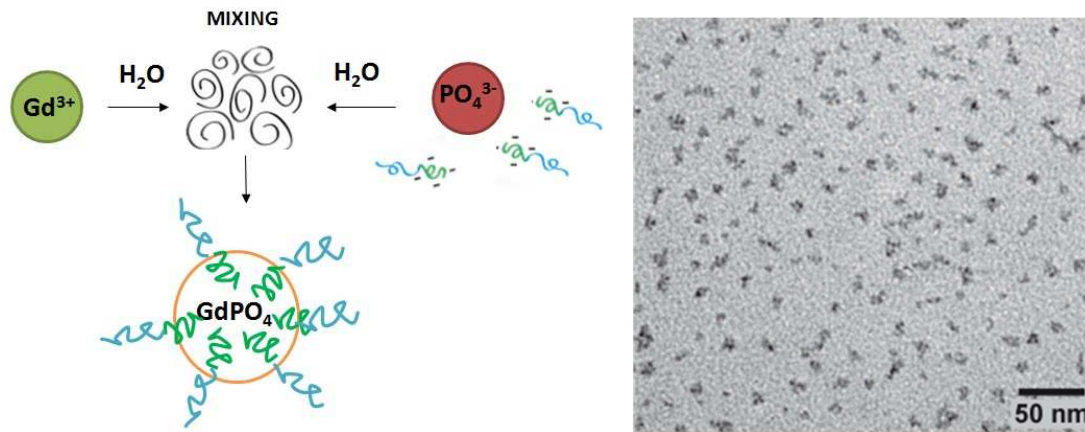


Figure 7. Left : Principle of the iFNP process, with the hydrophilic block copolymer in green and blue. Right : TEM images of GdPO_4 NPs obtained through nanoprecipitation process. Adapted from reference (Pinkerton et al., 2017).

Moreover to determine the relationship between particle size and relaxivity values, it is also necessary to be able to obtain particles of variable size but functionalized in an equivalent way. Lu et al. (2017) reported a simple and feasible approach to regulate NaGdF_4 NPs growth by changing the density of trisodium citrate chelator to obtain different sizes of NPs in the range of 100–220 nm. These nanoparticles of controlled size were then covered with a silica shell of similar thickness using a reverse microemulsion method. R_1 and r_2 relaxivity measurements of these $\text{NaGdF}_4@\text{SiO}_2$ NPs were investigated in water at 0.5 T and 7 T. At 0.5 or at 7 T, r_1 relaxivities decreased with the increase of particle size whereas r_2 values increased dramatically. Hence at 0.5 T particles with a diameter of 120 nm showed $r_1 = 1.4\text{ mM}^{-1}\cdot\text{s}^{-1}$ and $r_2 = 4.36\text{ mM}^{-1}\cdot\text{s}^{-1}$ whereas particles with a diameter of 250 nm showed $r_1 = 0.39\text{ mM}^{-1}\cdot\text{s}^{-1}$ and $r_2 = 8.55\text{ mM}^{-1}\cdot\text{s}^{-1}$. Interestingly the observed effect on r_2 was far more pronounced at higher field (7T). In addition, these $\text{NaGdF}_4@\text{SiO}_2$ NPs showed good compatibility and low cytotoxicity. This example demonstrated the primary interest in controlling particle size. Other examples proposed chemical recipes to obtain size controlled NPs with equivalent organic coating down to a few nm. Size-controlled GdPO_4 nanowires in a range of 120 ± 39 nm down to 6 ± 2 nm were synthesized in presence of hyperbranched polymers based on the polyamidoamine HyPAM in aqueous solutions and at room temperature.(Frangville, Gallois et al, 2016) As shown on Figure 8, relaxivity measurements of these hybrid materials showed a maximum for the 23 nm particle sample and revealed an optimal length at ca. 23 ± 11 nm for which promising r_1 and r_2 values were obtained ($r_1 = 55\pm 9$

$\text{mM}^{-1}\cdot\text{s}^{-1}$; $r_2 = 67 \pm 11 \text{ mM}^{-1}\cdot\text{s}^{-1}$). Hence a size dependence on measured r_1 and r_2 is observed with lower values of relaxivity for both larger and smaller particles.

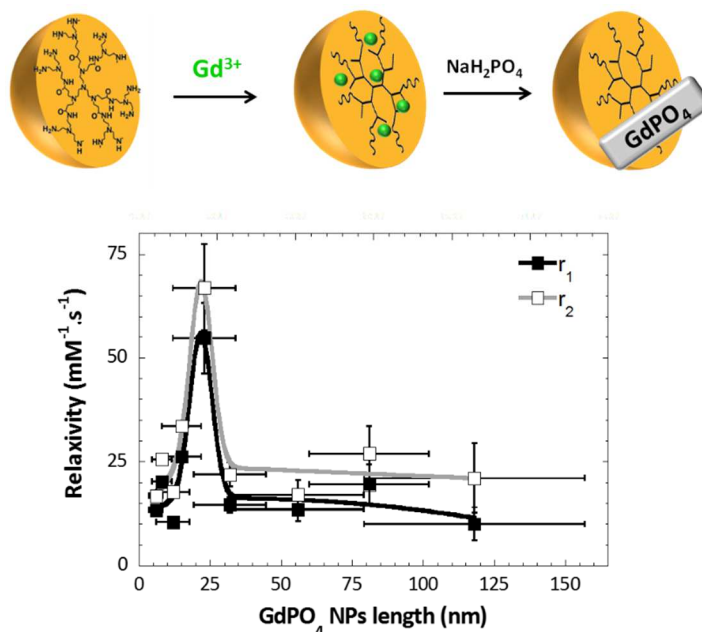


Figure 8. GdPO₄/HyPAM size dependence on r_1 and r_2 relaxivities (1.4 T). Particle lengths were determined before dialysis. Lines are guides to the eye. Adapted from (Frangville, Gallois et al, 2016).

Similar observations of an optimal particle size were observed for other particle systems, (Park et al., 2013; Wang et al., 2013) including NaGdF₄ and Gd₂O₃, and was attributed to contributing factors influencing relaxivity that have opposite particle size correlations. One influencing factor is the availability of Gd³⁺ ions at the surface, as direct chemical exchange of water molecules is the largest contributor to proton relaxation. The surface to volume ratio (S/V) increases as particle size gets smaller, accounting for the most often observed increase in relaxivity as particles become smaller. On the other hand, correlation times and therefore tumbling times are another factor. (Villaraza et al., 2010; Caravan, 2006; Johnson et al., 2011; Wiener et al., 1994) Tumbling times depend on the medium viscosity and hydrodynamic volume of the particles. If we assume the viscosity does not change for the different particle suspensions, then for a reasonable range of particle sizes, relaxivity should increase with hydrodynamic volume. For this serie with the same chemical coating, the apparent hydrodynamic diameter follows the same linear trend as the increase of NP length from ~10 to ~100 nm, allowing us to consider the NP length as the key parameter. These opposing contributions of surface area and hydrodynamic volume are then expected to give rise to an optimum particle size for any set of conditions. It is important to realize that correlation times will be affected by other parameters, such as medium viscosity and applied magnetic field strength, so any 'optimum' particle size will depend on the application. Furthermore, since the tumbling time depends on the hydrodynamic volume of the composite polymer-particle object, the polymer mediated preparation affords the potential

for tuning the response through synthetic variation of both the inorganic particle size and the thickness of the polymer coating.

2.2. Critical role of coating on relaxivity properties.

As we have just seen, the control of the nature and size of the inorganic part is of crucial importance to have access to nanoparticles with optimal relaxation properties for a given application. A second element playing on relaxivity values is the nature of the organic part covering the particles. The organic part surrounding the inorganic core performs several functions above its ability to control NPs growth during NPs synthesis.

Its primal role is to ensure that the particles have good colloidal stability in order to avoid any aggregation or precipitation phenomenon *in vivo*. For this purpose the use of organic shell comprising poly(ethylene glycol) (PEG) is of special interest as it minimizes adsorption of biomolecules onto the NPs and avoids fast clearance from blood system. Hence many works described the use of this polymer to cover inorganic NPs. For instance Lakew Mekuira *et al.* (2017) synthesized gadolinium oxide NPs covered with a dendrimer whose external functions were modified by PEG. The presence of PEG chains enhanced the biocompatibility, the circulation time in blood and the colloidal stability of the contrast agent. The leakage of Gadolinium ion was checked through absorbance measurements and also by titrating in PBS buffer for 120 hours and only a non-significant amount of Gd ions was released from this hybrid material. In addition, relaxivity values measured at a 7T magnetic field were very high for both r_1 and r_2 ($r_1=53.9 \text{ mM}^{-1}\cdot\text{s}^{-1}$ and $r_2=182.8 \text{ mM}^{-1}\cdot\text{s}^{-1}$) and compared very favorably to the one measured for Gd_2O_3 nanoparticles covered by different functionalized agent like PVP or single PEG chain (for these two systems relaxivities values equal to $r_1=12.1 \text{ mM}^{-1}\cdot\text{s}^{-1}$ and $r_2=33.2 \text{ mM}^{-1}\cdot\text{s}^{-1}$ and $r_1=4.4$ and $r_2=28.9 \text{ mM}^{-1}\cdot\text{s}^{-1}$ were found respectively).

In addition to stability property, this organic part enables to control the accessibility of water molecules in the vicinity of gadolinium and to confer colloidal stability to the hybrid material systems. Zheng *et al.* described the synthesis by a coprecipitation method of GdF_4 NPs with uniform morphology and narrow size distribution ($8.6\pm 1.1 \text{ nm}$). Then by using a two-step ligand exchange strategy, these nanoparticles were covered by different polymeric ligands: poly(ethylene glycol) (PEG), polyéthyleimine (PEI) and polyacrylic acid (PAA) (Zheng *et al.*, 2017). As illustrated in Figure 9, longitudinal (r_1) and transverse (r_2) relaxivities were found higher when NPs were covered by PAA group. Moreover when the average molecular weight of PAA used is changed (1200, 2000, 5000 or $8000 \text{ g}\cdot\text{mol}^{-1}$) optimal relaxivity values were found for PAA_{2000} . This result evidenced that strong surface ligand–water interaction can efficiently promote relaxivity. It is thus possible to develop ultrasmall Gd-dots with higher relaxation performance than CAs with bigger size. The called Gd-Dots were about 2.1 nm by size and then were more exposed to water, which explains the highest relaxivity value compared to other bigger nanoparticles. The promoting effect can be ascribed to the formation of second hydration shell, where the increased number of exchangeable water

molecules and their prolonged residence time result in an enhanced second-sphere contribution.

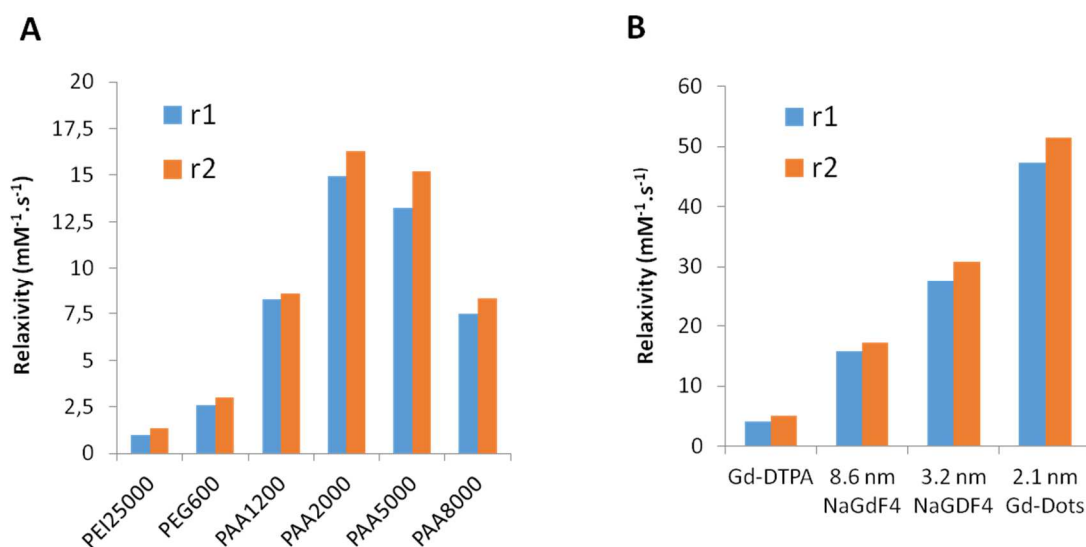


Figure 9. A. Longitudinal (r_1) and transverse (r_2) relaxivities of the samples measured at 0.5 T. Relaxivities of different samples measured at 0.5 T, including Gd-DTPA, PAA₂₀₀₀-capped NaGdF₄NPs (8.6 and 3.2 nm), and Gd-dots (2.1 nm). DLS analysis of the samples. Adapted from (Zheng et al., 2017).

Consequently, the choice of the structure of the organic part covering inorganic particles is of prior importance to obtain stable CAs with long residence time in vivo and high relaxivity values.

2.3. Toward multimodal agents.

By playing on both the nature of the inorganic and organic parts it is thus possible to obtain contrast agent NPs with multi-modal imaging or targeting properties. Nanoclusters containing both gold NPs and gadolinium ions were thus used as contrast agent for different imaging techniques Computed Tomography (CT), Near-Infrared Fluorescence (NIRF) and Magnetic Resonance (MR) imaging (Hou et al., 2017). These nanoclusters were stable through time with a hydrodynamic diameter of about 200 nm and the measured longitudinal relaxivity value r_1 was about 25 mM⁻¹·s⁻¹, which is about 5 times the one of the Gd-DTPA. Other examples described the introduction of luminescence properties on GdPO₄ NPs either by inserting Europium ions during the precipitation of gadolinium in presence of phosphate (Figure 10A) or by covering GdPO₄ NPs with luminescent molecules like indocyanine green or polymers bearing a fluorescent moiety (Figure 10B). (Pinkerton et al., 2018) Interestingly in the former case changing Gd/Eu ratio enabled also to enhance relaxivity properties of obtained NPs: higher relaxivity values were obtained with lower gadolinium content (Figure 10A).

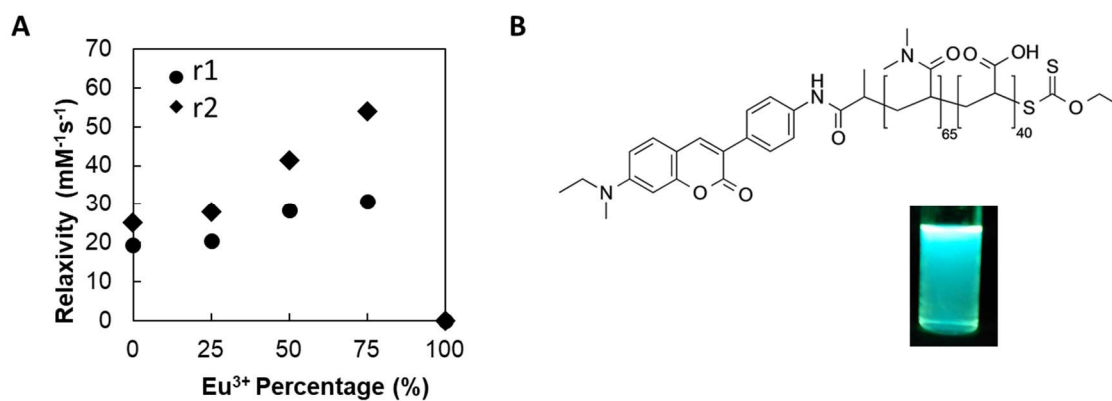


Figure 10. A. Relaxity values r_1 and r_2 of GdEuPO₄ NPs as a function of the Gd/Eu ratio. B. Structure of fluorescent polymer used as a functionalizing agent and picture of the resulting excited solution. Adapted from (Pinkerton et al., 2018).

Another combination of magnetic sensitivity and luminescence property was described by Maldiney et al. (2015) who worked on nanocrystals based on trivalent chromium-doped zinc gallate. Indeed, in the aim to get multimodal agents, Gd was added to these nanomaterials to both follow the luminescence of the agent and evaluate its relaxation properties. The nanoparticles were doped with Gd and showed higher relaxivity values with increasing Gd content (up to 4 mol%). With the idea to increase the residence time of the nanoparticles in the body, these ones were functionalized with poly(ethylene glycol) (PEG) chains through hydroxylation, condensation with amino-silanes and grafting of PEG_{5kDa}-NHS. This functionalization resulted in a higher contrast compared to a reference mouse. Additionally, it was evidenced that the uptake from the Kupffer cells in the liver was delayed, according to MR images, confirming the longer residence time.

Last but not least, active targeting remains one of the main applications of the synthesis of Gd-based nanoparticles. The contrast agents become then theranostic agents, used to give information about a precise area in the body, which is targeted. Ahmad et al. (2018) grafted on Gd₂O₃ nanoparticles with an average diameter about 2 nm, 5 commercial targeting probes composed of Arg-Gly-Asp peptides varying by the kind of amino acids present on the peptide chain, further named cyclic-RGDs. Grafting yield was between 40 and 50% and hydrodynamic diameter of the obtained nanohybrids was about 6 nm. Measured longitudinal relaxivities at 0.47 T and 25°C varied between 10 and 18 mM⁻¹·s⁻¹ which compared favorably to the ones of Gd-DTPA ($r_1 = 3.8$ mM⁻¹·s⁻¹) and Gd-DOTA ($r_1 = 4.2$ mM⁻¹·s⁻¹). This is explained with a stronger hydrophilicity of the cyclic-RGDs, raising the interaction with water molecules, and from a high quantity of Gd ions the surface of nanoparticle. *In vitro* internalization of one of the cyclic-RGD was made in U87MG tumor cells, showing the aggregation of nanoparticles on the cell surface after 24h of incubation. Finally *in vivo* experiments highlighted a higher contrast in tumoral areas compared to normal and necrosis parts, proving the efficient targeting of these nanoparticles towards tumor cells.

Conclusion. Developing new gadolinium based contrast agents is of tremendous importance with the aim to drastically limit the quantity of Gd ions remaining within the tissues and two challenges have to be tackled: decreasing the amount of Gd ions released and/or increasing the relaxivity properties of the Gd based CAs to limit the amount of injected compound. In this context, colloidal CAs are of special interest. Indeed the use of Gd-based colloidal structures in the 10 to 100 nm size range enables first to increase the relaxivity values of obtained CAs thanks to slower tumbling effect. The grafting or interaction of gadolinium complexes with other chemical structures such as nanodots, polymer with different architectures, liposomes or hybrid polyion complexes, helps to the formation of colloidal structures with improved relaxation properties. Furthermore, using inorganic nanoparticles (Gd_2O_3 , $GdPO_4$, $NaGdF_4$, GdF_3) instead of Gd complexes strengthens the stability of Gd within formed nanoparticle and thus limit the release of Gd ions *in vivo* and thus empowers the performance of Gd-based CAs at high magnetic fields. In addition, it is noteworthy to keep in mind that the properties of the inorganic particles are still dependent on the production of nanoparticles with well controlled size, morphology and appropriate coating. Lastly, playing with the composition of colloidal structures enables the insertion of additional features (targeting, fluorescence,...) that made them candidate of choice for new families of CAS with multimodal properties.

Acknowledgements. The authors gratefully acknowledge the CNRS, University Paul Sabatier and region Occitanie for financial support.

References

- Ahmad M.Y., Ahmad M.W., Cha H., Oh I-T., Tegafaw T., Miao X., Ho S.L., Marasini S., Ghazanfari A., Yue H., Ryeom H-K., Lee J., Chae K.S., Chang Y., Lee G.H., 2018, Cyclic RGD-Coated Ultrasmall Gd_2O_3 Nanoparticles as Tumor-Targeting Positive Magnetic Resonance Imaging Contrast Agents, *Eur. J. Inorg. Chem.*, 3070-379, DOI: 10.1002/ejic.201800023
- Bridot, J.-L., Faure, A.-C., Laurent, S., Rivière, C., Billotey, C., Hiba, B., Janier, M., Josserand, V., Coll, J.-L., Elst, L.V., Muller, R., Roux, S., Perriat, P., and Tillement, O., 2007, Hybrid gadolinium oxide nanoparticles: multimodal contrast agents for *in vivo* imaging, *J. Am. Chem. Soc.*, 129, 5076. DOI: 10.1021/ja068356j
- Bryant, L.H., Brechbiel, M.W., Wu, C., Bulte, J.W., Herynek, V., Frank, J.A., 1999, Synthesis and relaxometry of high-generation (G=5, 7, 9, and 10) PAMAM dendrimer-DOTA-gadolinium chelates, *Magn. Reson. Imaging* 9, 348-352. DOI: [https://doi.org/10.1002/\(SICI\)1522-2586\(199902\)9:2<348::AID-JMRI30>3.0.CO;2-J](https://doi.org/10.1002/(SICI)1522-2586(199902)9:2<348::AID-JMRI30>3.0.CO;2-J)
- Cao F., Huang, T., Wang, Y., Liu, F., Chen, L., Ling, J. and Sun, J., 2015, Novel lanthanide-polymer complexes for dye-free dual modal probes for MRI and fluorescence imaging, *Polym. Chem.*, 6, 7949-7957. DOI: 10.1039/C5PY01011J
- Caravan, P., 2006, Strategies for increasing the sensitivity of gadolinium based MRI contrast agents., *Chem. Soc. Rev.* 35, 512. DOI: 10.1039/b510982p

- Cheng, Y., Morshed, R., Auffinger, B., Tobias A. L., and Lesniak, M. S., 2014, Multifunctional nanoparticles for brain tumor imaging and therapy, *Adv. Drug Deliv. Rev.* 66, 42. DOI: 10.1016/j.addr.2013.09.006
- Cheng, Z., Dai, Y., Kang, X., Li, C., Huang, S., Lian, H., Hou, Z., Ma, P., and Lin, J., 2014, Gelatin-encapsulated iron oxide nanoparticles for platinum (IV) prodrug delivery, enzyme-stimulated release and MRI, *Biomaterials*, 35, 6359. DOI: 10.1016/j.biomaterials.2014.04.029
- Colosimo, C., Ruscalleda, J., Korves, M., La Ferla, R., Wool, C., Pianezzola, P., Kirchin, M. A., 2001, Detection of Intracranial Metastases: A Multicenter Inpatient Comparison of Gadobenate Dimeglumine-Enhanced MRI with Routinely Used Contrast Agents at Equal Dosage, *Invest. Radiol.* 36, 72.
- Das, G. K., Heng, B. C., Ng, S-C., White, T., Loo, J. S. C., D'Silva, L., Padmanabhan, P., Bhakoo, K. K., Selvan, S. T., and Tan, T. T. Y., 2010, Gadolinium Oxide Ultrathin Nanorods as Multimodal Contrast Agents for Optical and Magnetic Resonance Imaging, *Langmuir*, 26, 8959. DOI: 10.1021/la904751q
- Das, T., Sharma, A., Talukder, G., 1988, Effects of lanthanum in cellular systems, *Biol Trace Elem. Res.*, 18, 201. DOI: 0163-4984/88/1800-0201 \$05.60
- Ding, C., Zhu, A., Tian, Y., 2014, Functional Surface Engineering of C-Dots for fluorescent Biosensing and in vivo Bioimaging, *Acc. Chem. Res.*, 47, 20 DOI: 10.1021/ar400023s
- Du, Q., Huang, Z., Wu, Z., Meng, X., Yin, G., Gao, F., and Wang, L., 2015, Facile preparation and bifunctional imaging of Eu-doped GdPO₄ nanorods with MRI and cellular luminescence, *Dalton Trans.*, 44, 3934. DOI: 10.1039/C4DT03444A
- Du, Y., Qian, M., Li, C., Jiang, H., Yang, Y., Huang, R., 2018, Facile marriage of Gd³⁺ to polymer-coated carbon nanodots with enhanced biocompatibility for targeted MR/fluorescence imaging of glioma, *Int. J. Pharm.*, 552, 84-90. DOI: <https://doi.org/10.1016/j.ijpharm.2018.09.010>
- Dumont, M. F., Baligand, C., Li, Y., Knowles, E. S., Meisel, M. W., Walter, G. A., and Talham, D. R., 2012, DNA surface modified gadolinium phosphate nanoparticles as MRI contrast agents, *Bioconjug. Chem.*, 23, 951. DOI: 10.1021/bc200553h
- Elorza, V., 1969, Toxicity of metallic ions to *Aspergillus nidulans*, *Microbiol. Esp.*, 22, 131.
- Essig, M., 2005, Gadobenate dimeglumine (MultiHance®) in MR imaging of the CNS: Studies to assess the benefits of a high relaxivity contrast agent, *Acad. Radiol.*, 12 Suppl 1, S23. DOI: 10.1016/j.acra.2005.02.020
- Evanics, F., Diamente, P.R., Veggel, F. C. J. M., Van Stanisz, G. J., and Prosser, R. S., 2006, Water-Soluble GdF₃ and GdF₃/LaF₃ Nanoparticles – Physical Characterization and NMR Relaxation Properties, *Chem. Mater.*, 18, 2499. DOI: 10.1021/cm052299w

Fang, Y.-P., Xu, A.-W., Song, R.-Q., Zhang, H.-X., You, L.-P., Yu, J. C., Liu, H.-Q., 2003, Systematic synthesis and characterization of single-crystal lanthanide orthophosphate nanowires, *J. Am. Chem. Soc.*, 125, 16025. DOI: 10.1021/ja037280d

Faucher, L., Tremblay, M., Lagueux, J., Gossuin, Y., and Fortin, M.-A., 2012, Rapid synthesis of PEGylated ultrasmall gadolinium oxide nanoparticles for cell labeling and tracking with MRI, *ACS Appl. Mater. Interfaces*, 4, 4506. DOI: 10.1021/am3006466

Frangville, C., Gallois, M., Li, Y., Nguyen, H.H., Lauth-de Viguerie, N., Talham, D.R., Mingotaud, C. and Marty, J-D. 2016, Hyperbranched polymer mediated size-controlled synthesis of gadolinium phosphate nanoparticles: colloidal properties and particle size-dependence on MRI relaxivity, *Nanoscale*, 2016, 8, 4252-4259, DOI: 10.1039/c5nr05064b

Frangville, C., Li, Y., Billotey, C., Talham, D.R., Taleb, J., Roux, P., Marty, J-D. and Mingotaud, C., 2016, Assembly of Double-Hydrophilic Block Copolymers Triggered by Gadolinium Ions: New Colloidal MRI Contrast Agents, *Nano Lett.*, 16, 4069–4073. DOI: 10.1021/acs.nanolett.6b00664

Gibby, W. A., Gibby, K. A. , Gibby, W. A., 2004, Gadolinium tissue deposition in brain and bone, *Invest. Radiol.*, 39, 138. DOI: 10.1016/j.mri.2016.08.025

Harpur, E. S., Worah, D., Hals, P. A., Holtz, E., Furuham, K., Nomura, H., 1993, Preclinical Safety Assessment and Pharmacokinetics of Gadodiamide Injection, a New Magnetic Resonance Imaging Contrast Agent, *Invest. Radiol.*, 28 Suppl 1, S28. 10.1097/00004424-199303001-00004

Hermann, P., Kotek, J., Kubicek, V., and Lukes, I., 2008, Gadolinium(III) complexes as MRI contrast agents: ligand design and properties of the complexes, *Dalton Trans.*, 3027–3047 DOI: 10.1039/B719704G

Hifumi, H., Yamaoka, S., Tanimoto, Akatsu, T., Shindo, Y., Honda, A., Citterio, D., Oka, K., Kuribayashi, S., and Suzuki, K., 2009, Dextran Coated Gadolinium Phosphate Nanoparticles for Magnetic Resonance Tumor Imaging, *J. Mater. Chem.*, 19, 6393. DOI: 10.1039/B902134E

Hifumi, H., Yamaoka, S., Tanimoto, A., Citterio D., and Suzuki, K., 2006, Gadolinium-based Hybrid Nanoparticles as a Positive MR Contrast Agent, *J. Am. Chem. Soc.*, 128, 15090. DOI: 10.1021/ja066442d

Hikichi, Y., Hukuo, K., and Shiokawa, J., 1978, Syntheses of Rare Earth Orthophosphates, *Bull. Chem. Soc. Jpn.*, 51, 3645. DOI: 10.1246/bcsj.51.3645

Hou, W., Xia, F.,Alfranca, G., Yan, H., Zhi, X., Liu, Y., Peng, C., Zhang, C., Martinez de la Fuente, J., et Cui, D., 2017, Nanoparticles for multi-modality cancer diagnosis: simple protocol for self-assembly of gold nanoclusters mediated by gadolinium ions, *Biomaterials*, 12,103-114. DOI: 10.1016/j.biomaterials.2016.12.027

Johansson, L., Kirchin, M. A., Ahlström, H., 2012, Gadobenate Dimeglumine (Multihance) in Mr Angiography: An In-Vitro Phantom Comparison with Gadopentetate Dimeglumine (Magnevist) at Different Concentrations, *Acta Radiol.*, 53, 1112. DOI: 10.1258/ar.2012.120181

Johnson, N. J. J., Oakden, W., Stanisiz, G. J., Prosser, R. S., Van Veggel, F. C. J. M., 2011, Size-Tunable, Ultrasmall NaGdF₄ Nanoparticles: Insights into Their T₁ MRI Contrast Enhancement., *Chem. Mater.*, 23, 3714. DOI: 10.1021/cm201297x

Kabalka, G., Buonocore, E., Hubner, K., Moss, T., Norley, N., Huang, L., 1987, Gadolinium-labeled liposomes: targeted MR contrast agents for the liver and spleen, *Radiology*, 163, 255-258 DOI : 10.1148/radiology.163.1.3454163

Kanda, T., Fukusato, T., Matsuda, M., Toyoda, K., Oba, H., Kotoku, J., Haruyama, T., Kitajima, K., Furui, S., 2015, Gadolinium-based Contrast Agent Accumulates in the Brain Even in Subjects without Severe Renal Dysfunction: Evaluation of Autopsy Brain Specimens with Inductively Coupled Plasma Mass Spectroscopy, *Radiology*, 276, 228. DOI: 10.1148/radiol.2015142690

Kanda, T., Ishii, K., Kawaguchi, H., Kitajima, K., Takenaka, D., 2014, High signal intensity in the dentate nucleus and globus pallidus on unenhanced T1-weighted MR images: relationship with increasing cumulative dose of a gadolinium-based contrast material, *Radiology*, 270, 834. DOI: 10.1148/radiol.13131669

Kanda, T., Osawa, M., Oba, H., Toyoda, K., Kotoku, J., Haruyama, T., Takeshita, K., Furui, S., 2015, High Signal Intensity in Dentate Nucleus on unenhanced T1-weighted MR Images: Association with Linear versus Macrocyclic Gadolinium Chelate Administration, *Radiology*, 275, 803. DOI: 10.1148/radiol.14140364

Lakew Mekuria, S., Ayane Debele, T. and Tsai, H.-C., 2017, Encapsulation of Gadolinium Oxide Nanoparticle (Gd₂O₃) Contrasting Agents in PAMAM Dendrimer Templates for Enhanced Magnetic Resonance Imaging in Vivo, *ACS Appl. Mater. Interfaces*, 9, 6782–6795. DOI: 10.1021/acsami.6b14075

Laudise, R. A., and Ballman, A. A., 1958, Hydrothermal Synthesis of Sapphire, *J. Am. Chem. Soc.*, 80, 2655. DOI: 10.1021/ja01544a014

Lessing, P. and Erickson, A.W., 2003, Synthesis and characterization of gadolinium phosphate neutron absorber, *J. Eur. Ceram. Soc.*, 23, 3049. DOI: 10.1016/S0955-2219(03)00100-6

Li, Y., Beija, M., Laurent, S., Vander Elst, L., Muller, R.N., Duong, H.T., Lowe, A.B., Davis, T.P. and Boyer, C., 2012, Macromolecular Ligands for Gadolinium MRI Contrast Agents, *Macromolecules*, 45, 4196-4204. DOI: 10.1021/ma300521c

Li, R., Ji, Z., Chang, C. H., Dunphy, D. R., Cai, X., Meng, H., Zhang, H., Sun, B., Wang, X., Dong, J., Lin, S., Wang, M., Liao, Y.-P., Brinker, C. J., Nel A. and Xia T., 2014, Surface Interactions with Compartmentalized Cellular Phosphates Explain Rare Earth Oxide Nanoparticle Hazard and Provide Opportunities for Safer Design, *ACS Nano*, 8, 1771-1783. DOI: 10.1021/nn406166n.

Liu, X., and Byrne, R. H., 1997, Rare earth and yttrium phosphate solubilities in aqueous solution, *Geochim. Cosmochim. Acta*, 61, 1625. DOI: 10.1016/S0016-7037(97)00037-9

Lu, Z., Deng, R., Zhen, M., Li, X., Zou, T., Zou, Y., Guan, M., Zhang, Y., Wang, Y., Yu, T., Shu, C., and Wang, C., 2017, Size-tunable NaGdF₄ nanoparticles as T₂ contrast agents for high-field magnetic resonance imaging, *RSC Adv.*, 7, 43125. DOI: 10.1039/C7RA08303C

Maldiney T., Doan B-T., Alloyeau D., Bessodes M., Scherman D., Richard C., 2015, Gadolinium-Doped Persistent Nanophosphors as Versatile Tool for Multimodal In Vivo Imaging, *Adv. Funct. Mater.*, 25, 331-338, DOI: 10.1002/adfm.201401612

Mansfield, P., Maudsley, A. A., 1976, Line scan proton spin imaging in biological structures by NMR, *Phys. Med. Biol.*, 21, 847. DOI: 10.1088/0031-9155/21/5/013

Margeruma, Lawrence D., Campion, Brian K., Koo, M., Shargill, N., Lai, J-J., Marumoto, A., Sontum, Per C., 1997, Gadolinium(III) DO3A macrocycles and polyethylene glycol coupled to dendrimers – Effect of molecular weight on physical and biological properties of macromolecular magnetic resonance imaging contrast agents, *J. Alloys Compd.*, 249, 185-190. DOI: 10.1016/S0925-8388(96)02830-7

Mingotaud, C., Marty, J.-D., Frangville, C., Talham, D.R., 2017, Agents de contraste pour imagerie medicale, FR3043330 - 2017-05-12 (BOPI 2017-19)

Park, J. Y., Baek, M. J., Choi, E.S., Woo, S., Kim, J.H., Kim, T.J., Jung, J.C., Chae, S., Chang, Y., and Lee, G. H., 2009, Paramagnetic ultrasmall gadolinium oxide nanoparticles as advanced T1 MRI contrast agent: account for large longitudinal relaxivity, optimal particle diameter, and in vivo T1 MR images., *ACS Nano*, 3, 3663-9. DOI: 10.1021/nn900761s

Patten, R. M., Lo, S. K., Phillips, J. J., Bowman, S. C., Glazer, G.M., Wall, S. D., Bova, J. G., Harris, R. D., Wheat, R. L., Johnson, C. D., 1993, Positive bowel contrast agent for MR imaging of the abdomen: phase II and III clinical trials., *Radiology*, 189 (1), 277-283. DOI: 10.1148/radiology.189.1.8372205

Pinkerton, N.M., Behar, L., Hadri, K., Amouroux, B., Mingotaud, C., Talham, D.R., Chassaing, S., and Marty, J.-D., 2017, Ionic Flash Nanoprecipitation (iFNP) for the facile, one-step synthesis of inorganic-organic hybrid nanoparticles in water, *Nanoscale* 9, 1403-1408. DOI: 10.1039/c6nr09364g

Pinkerton, N.M., Behar, L. Hadri, K., Amouroux, B., Mingotaud, C., Talham, D.R., Chassaing S., and Marty, J.-D., 2017 Quench ionic flash nano precipitation as a simple and tunable

approach to decouple growth and functionalization for the one-step synthesis of functional LnPO_4 -based nanoparticles in water., *Chem. Commun.*, 2018, 54, 9438-9441. DOI: 10.1039/C8CC04163F.

Radbruch, A., Weberling, L. D., Kieslich, P. J., Eidel, O., Burth, S., Kickingereeder, P., Heiland, S., Schmiedl, W.U., Moseley, M. E., Ogan, M. D, Chew, W. M., Brasch, R. C., 1987, Gadolinium Retention in the Dentate Nucleus and Globus Pallidus is Dependent on the Class of Contrast Agent., *J. Comput. Assist. Tomogr.*, 11, 306. DOI: 10.1148/radiol.2015150337

Radbruch, A., Weberling, L. D., Kieslich, P. J., Eidel, O., Burth, S., Kickingereeder, P., Heiland, S., Schmiedl, W.U., Moseley, M. E., Ogan, M. D, Chew, W. M., Brasch, R. C., 1987, Gadolinium Retention in the Dentate Nucleus and Globus Pallidus is Dependent on the Class of Contrast Agent., *J. Comput. Assist. Tomogr.*, 11, 306. DOI: 10.1148/radiol.2015150337

Ren, W., Tian, G., Zhou, L., Yin, W., Yan, L., Jin, S., Zu, Y., Li, S., Gu, Z., and Zhao, Y., 2012, Mn^{2+} dopant-controlled synthesis of $\text{NaYF}_4:\text{Yb}/\text{Er}$ upconversion nanoparticles for in vivo imaging and drug delivery, *Nanoscale*, 4, 3754. DOI: 10.1002/adma.201104741

Rodriguez-Liviano, S., Becerro, A. I., Alcántara, D., Grazú, V., de la Fuente, J. M., and Ocaña, M., 2013, Synthesis and properties of multifunctional tetragonal $\text{Eu}:\text{GdPO}_4$ nanocubes for optical and magnetic resonance imaging applications, *Inorg. Chem.*, 52, 647. DOI: 10.1021/ic3016996

Sieber, M. A., Lengsfeld, P., Frenzel, T., Golfier, S., Schmitt-Willich, H., Siegmund, F., Walter, J., Weinmann, H.-J., Pietsch, H., 2008, Gadolinium-based contrast agents and their potential role in the pathogenesis of nephrogenic systemic fibrosis: the role of excess ligand, *Eur. Radiol.*, 18, 2164. DOI: 10.1002/jmri.21368

Schmiedl, U., Moseley M. E., Ogan M. D., Chew W. M., Brasch R.C., 1987, Comparison of initial biodistribution patterns of Gd-DTPA and albumin-(Gd-DTPA) using rapid spin echo MR imaging. *J. Comput. Assist. Tomogr.*, 11(2), 306-313.

Skupin-Mrugalska P., Sobotta L., Warowicka A., Wereszczynska B., Zalewski T., Gierlich P., Jarek M., Nowaczyk G., Kempka M., Gapinski J., Jurga S., Mielcarek J., 2018, Theranostic liposomes as a bimodal carrier for magnetic resonance imaging contrast agent and photosensitizer, *Journal of Inorganic Biochemistry*, 180, 1-14, DOI: 10.1016/j.jinorgbio.2017.11.025

Tran, V.L., Thakare, V., Natuzzi, M., Moreau, M., Oudot, A., Vrigneaud, J-M., Courteau, A., Louis, C., Roux, S., Boschetti, F., Denat, F., Tillement, O., and Lux, F., 2018, Functionalization of Gadolinium Chelates Silica Nanoparticle through Silane Chemistry for Simultaneous MRI/ ^{64}Cu PET Imaging, *Hindawi, Contrast Media & Molecular Imaging* Volume Article ID 7938267, 10 pages. DOI: 10.1155/2018/7938267

Villaraza, A.J. L., Bumb, A. and Brechbiel, M. W., 2010, *Macromolecules, Dendrimers, and*

Nanomaterials in Magnetic Resonance Imaging: The Interplay between Size, Function and Pharmacokinetics, *Chem. Rev.*, 110, 2921–2959. DOI: 10.1021/cr900232t

Wang J., Velders A.H, Gianolio, E., Aime, S., Vergeldt, F.J, Van as, H. Yan, Y., Drechsler, M., de Keiser, A., Cohen Stuart, M.A. and van der Gucht, J., 2013, Controlled mixing of lanthanide(III) ions in coacervate core micelles, *Chem. Commun.*, 49, 3736-3738.. DOI: 10.1039/C3CC39148E

Wang, J., Cohen Stuart, M. A., Marcelis, A. T. M., Colomb-Delsuc, M., Otto, S., and van der Gucht, J., 2012, Stable polymer micelles formed by metal coordination, *Macromolecules*, 45,7179-7185. DOI: 10.1021/ma301323z

Wang, J., Marleen de Kool, R.H., and Velders, A.H., 2015, Lanthanide-Dipicolinic Acid Coordination Driven Micelles with Enhanced Stability and Tunable Function, *Langmuir*, 31, 12251-12259. DOI: 10.1021/acs.langmuir.5b03226

Weinmann, H. J., Brasch, R. C., Press, W. R., Wesbey, G. E., 1984, Characteristics of gadolinium-DTPA complex: A Potential NMR contrast agent, *AJR Am. J. Roentgenol.*, 142, 619-624. DOI : 10.2214/ajr.142.3.619

Wiener, E., Brechbiel, M. W., Brothers, H., Magin, R. L., Gansow, O. A., Tomalia, D. .A., and Lauterbur, P. C. , 1994, Dendrimer-based metal chelates: A new class of magnetic resonance imaging contrast agents. *Magn. Reson. Med.*, 31, 1. DOI: 10.1002/mrm.1910310102

Xu, J., Gai, S., Ma, P., Dai, Y., Yang, G., He, F., and Yang, P., 2014, Gadolinium fluoride mesoporous microspheres: Controllable synthesis, materials and biological properties, *J. Mater. Chem. B*, 2, 1791. DOI: 10.1039/C3TB21465F

Yoo S.P., Pineda F., Barrett J.C., Poon C., Tirrell M., Chung E.J., 2016, Gadolinium-Functionalized Peptide Amphiphile Micelles for Multimodal Imaging of Atherosclerotic Lesions, *ACS Omega*, 1, 996-1003, DOI: [10.1021/acsomega.6b00210](https://doi.org/10.1021/acsomega.6b00210)

Young, I. R., Clarke, G. J., Bailes, D. R., Pennock, J. M., Doyle, F. H., Bydder, G. M., 1981, Enhancement of relaxation rate with paramagnetic contrast agents in NMR imaging, *J Comput Tomogr* 5, 543. DOI: [https://doi.org/10.1016/0149-936X\(81\)90089-8](https://doi.org/10.1016/0149-936X(81)90089-8)

Younis, M., Darcos, V., Paniagua, C., Ronjat, P., Lemaire, L., Nottelet, B., Garric, X., Bakkour, Y., El Nakat, J. H., and Coudane, J., 2016, MRI-visible polymer based on poly(methyl methacrylate) for imaging applications, *RSC Adv.*, 6, 5754-5760. DOI: 10.1039/C5RA23646K

Zheng, X., Zhao, K., Tang, J., Wang, X-Y., Li, L-D., Chen, N-X., Wang, Y-J., Shi, S., Zhang, X. Malaisamy, S., Sun, L-D., Wang, X., Chen, C., and Yan, C-H., 2017, Gd-Dots with Strong Ligand-Water Interaction for Ultrasensitive Magnetic Resonance Renography. *ACS Nano*, 11, 3642–3650. DOI: 10.1021/acsnano.6b07959